ACE2-Targeting Monoclonal Antibody As A "Pan" Coronavirus Blocker *In Vitro* and In A Mouse Model

Yuning Chen[1,7,*], Yanan Zhang[2,7,*], Renhong Yan[3,*], Guifeng Wang[1], Yuanyuan Zhang[3], Zherui Zhang[2,7], Yaning Li[5], Wendi Chu[1], Yili Chen[4], Ganjun Chen[4,7], Qi Wang[1], Qiang Zhou[3]†, Bo Zhang[2,6]†, Chunhe Wang[1,4]†

Affiliations:

[1]Biotherapeutics Discovery Research Center, Shanghai Institute of Materia Medica, Chinese Academy of Sciences, Shanghai 200126, China.

[2]Key Laboratory of Special Pathogens and Biosafety, Wuhan Institute of Virology, Center for Biosafety Mega-Science, Chinese Academy of Sciences, Wuhan, Hubei 430071, China.

[3]Center for Infectious Disease Research, Westlake Laboratory of Life Sciences and Biomedicine, Key Laboratory of Structural Biology of Zhejiang Province, School of

Life Sciences, Westlake University, and Institute of Biology, Westlake Institute for Advanced Study, 18 Shilongshan Road, Hangzhou, Zhejiang 310024, China.

[4]Dartsbio Pharmaceuticals, Zhongshan, Guangdong 528400, China

[5]Beijing Advanced Innovation Center for Structural Biology, Tsinghua-Peking Joint Center for Life Sciences, School of Life Sciences, Tsinghua University, Beijing 100084, China.

[6]Drug Discovery Center for Infectious Disease, Nankai University, Tianjin 300350, China

[7]University of Chinese Academy of Sciences, Beijing 100049, China;

***These authors contributed equally to this work.**

† Corresponding to: Chunhe Wang (wangc@simm.ac.cn), Bo Zhang (zhangbo@wh.iov.cn) or Qiang Zhou (zhouqiang@westlake.edu.cn).

Abstract

Coronaviruses have caused three major outbreaks of infectious disease since the beginning of 21st century. Broad-spectrum strategies that can be utilized in both current and future coronavirus outbreaks and mutation-tolerant are sought after. Here we report a monoclonal antibody 3E8 targeting human angiotensin-converting enzyme 2 (ACE2) neutralized pseudo-typed coronaviruse SARS-CoV-2, SARS-CoV-2-D614G, SARS-CoV and HCoV-NL63, without affecting physiological activities of ACE2 or causing toxicity in mouse model. 3E8 also blocked live SARS-CoV-2 infection *in vitro* and in a mouse model of COVID-19. Cryo-EM studies revealed the binding site of 3E8 on ACE2 and identified Histone 34 of ACE2 as a critical site of anti-viral epitope. Overall, our work has provided a potential "pan" coronavirus management strategy and disclosed a "pan" anti-coronavirus epitope on human ACE2 for the first time.

Summary: Blocking Multiple Coronaviruses by An ACE2-Neutralizing Monoclonal Antibody

Main Text

In the last 20 years, coronaviruses have cyclically caused three major infectious outbreaks in human, including severe acute respiratory syndrome (SARS) (*1*), Middle East respiratory syndrome (MERS) (*2*), and coronavirus disease 2019 (COVID-19) (*3, 4*). It is possible that future outbreaks are caused by not yet discovered coronaviruses. To treat COVID-19 and prepare for future coronavirus outbreaks, broad-spectrum coronavirus controlling strategies are sought after. So far, only small molecule drug remdesivir with broad (in theory) but marginal efficacies has been approved for treating COVID-19 (*5, 6*), the latest pandemic caused by severe acute respiratory syndrome coronavirus 2 (SARS-CoV-2). No drugs with conclusive benefits have ever been approved for SARS or MERS.

Coronaviruses are highly glycosylated and mutate frequently. For example, analyses of over 28,000 gene sequences of SARS-CoV-2 spike protein (S-protein) in May 2020 revealed a D614G amino acid substitution (SARS-CoV-2-D614G) that was rare before March 2020, but increased greatly in frequency as the pandemic spread worldwide, reaching over 74% of all published sequences by June 2020(*7*). Frequent

mutation renders coronaviruses the ability to evade single target-specific medications easily (*8, 9*). In theory, broad-spectrum coronavirus drugs have the best chance to withstand viral mutations and offer patients long-term benefits.

The key to develop broad-spectrum coronavirus therapeutics is to identify broad-spectrum druggable and specific anti-viral targets. Remdesivir interferes with the action of viral RNA-dependent RNA polymerase and evades proofreading by viral exoribonuclease, causing decrease in viral RNA production (*5, 6*). Although RNA polymerase is a broad anti-RNA virus target, it suffers from low specificity and efficacy. Recently, a peptide, named P9R, has been demonstrated to have broad antiviral activities against respiratory viruses including influenza virus and SARS-CoV-2, but it is a general immunosuppressant and not coronavirus specific (*10*). By employing a multi-dimensional approach, Gordon et al. proposed a set of potential “pan” viral target for coronaviruses, but the druggability of these targets are yet to be evaluated (*11*).

The entry of SARS-CoV-2 into host cells is triggered by binding of their envelope spike glycoproteins (S-protein) to angiotensin-converting enzyme 2 (ACE2) molecules expressed on host cells (*12, 13*). The S-protein consists of two subunits: 1) S1-subunit

(also called S1-protein) at N-terminal containing the receptor-binding domain (RBD) that is responsible for ACE2 binding; 2) S2-subunit at C-terminal responsible for membrane fusion (*13*). Due to its importance in viral entry, the RBD of SARS-CoV-2 has been heavily targeted by antibodies as well as small molecule approaches (*14-18*), but RBD-targeting approaches in general are not broad spectrum due to the diversity of RBD sequences.

ACE2 is a type-I transmembrane glycoprotein that plays important roles in maintaining blood pressure homeostasis in the renin-angiotensin system (*19, 20*). Mysteriously, it serves as the shared receptor in human and several other host species for multiple coronaviruses, including SARS-CoV-2, SARS-CoV and HCoV-NL63, etc. (*12, 21, 22*). SARS-CoV, a close sibling of SARS-CoV-2 in coronavirus family, was the culprit that caused the prior coronavirus outbreak in 2003 (*3*), while HCoV-NL63 infects human much more frequently but usually causes only cold symptoms with moderate clinical impacts (*23*). Binding of coronavirus to ACE2 not only facilitates viral entry into the host cells, but also down-regulates ACE2 expression (*24, 25*). Previous results revealed that RBD binding site of ACE2 does not overlap with its

catalytic site (*26-28*), it is therefore hypothesized that targeting ACE2 with neutralizing antibodies can block the entry of all ACE2-dependent coronaviruses, while sparing ACE2's physiological activities. Such antibodies can, in theory, be utilized in managing both current and future coronavirus outbreaks and tolerate viral mutations. By targeting ACE2, additionally, the antibody could be evaluated in HCoV-NL63 patients even when COVID-19 patients are no longer available for clinical trials. To test our hypothesis, we generated an ACE2-targeting monoclonal antibody, namely 3E8, to neutralize S1/ACE2 interactions. The therapeutic potentials and safety profiles of 3E8 were investigated and the key binding sites of 3E8 on human ACE2 molecule were revealed by cyro-EM to aid future drug discovery endeavor.

BALB/c mice were immunized with Fc-tagged human ACE2 protein and the sera were screened for binding to ACE2 (Fig. S1A) and blocking SARS-CoV-2-S1-subunit/ACE2 interaction (Fig. S1B). Hybridoma cells were constructed and the supernatants were screened by ACE2 binding and S1-subunit blocking. Antibody 3E8 was selected from a pool of neutralizing antibodies as the most efficacious blocker of S1-subunit/ACE2 binding. The variable regions of the heavy (VH)

and light (VL) chains were cloned into human IgG4 backbone, transiently expressed in HEK293F cells and purified (Fig. S1C).

We then measured the binding affinity of 3E8 to His-tagged human ACE2 protein with ELISA and biolayer interferometry (BLI). The EC_{50} value was 15.35 nM in ELISA (Fig. 1A) and dissociation constant (KD) was 32.6 nM in BLI (Fig. 1B). It also bound to HEK293F cells ectopically overexpressing human ACE2 and Vero E6 cells endogenously expressing human ACE2, as demonstrated by flow cytometry (Fig. S1D).

We next investigated the ability of 3E8 to neutralize S1-subunit/ACE2 interaction. S1-subunits from SARS-CoV-2-D614G, SARS-CoV-2 (D614), SARS-CoV and HCoV-NL63 were included. SARS-CoV-2-D614G and SARS-CoV-2 represent 64.6% and 30% respectively of all analyzed SARS-CoV-2 sequences in GISAID database. The EC_{50} values of S1-subunits from different coronaviruses (Fig. 1C and Fig. S1E) to His-tagged recombinant human ACE2 molecule were 2.58, 11.82, 1.13 and 24.24 nM, respectively (Fig. 1E). Incubation with 3E8 effectively neutralized all S-subunit binding to ACE2 (Fig. 1D) and the IC_{50} values were 13.80, 7.12, 13.73 and 4.96 nM, respectively

(Fig. 1E). Thus, 3E8 can broadly neutralize the binding of S1-subunits from 4 different multiple coronaviruses to human ACE2 molecules.

To further test our hypothesis, we constructed pseudo-typed coronaviruses with full-length S-proteins from SARS-CoV-2-D614G, SARS-CoV-2, SARS-CoV and HCoV-NL63. All pseudoviruses could infect HEK293F cells that ectopically express human ACE2, while SARS-CoV-2-D614G showed significantly-enhanced infectivity when compared to the original SARS-CoV-2 (D614) (Fig. S2). Incubation with 3E8 fully abolished the infectivity of all pseudoviruses, with IC_{50} values at 0.13, 0.07, 0.24 and 1.06 nM, respectively (Fig. 2, A, C). In comparison, B38, a SARS-CoV-2 RBD-targeting antibody currently under clinical development (*29*), could only suppress the infectivity of SARS-CoV-2-D614G and SARS-CoV-2, but not SARS-CoV or HCoV-NL63. The suppression of 3E8 was not only broader, but also remarkably more efficacious and potent, as the EC_{50} values of 3E8 was 230- and 618-fold improved when compared to B38 in neutralizing SARS-CoV-2-D614G and SARS-CoV-2 (Fig. 2C). ACE2-Fc, a virus RBD-targeting fusion protein consisting human ACE2 extracellular domain and the Fc region of human IgG1, showed broad but mediocre blocking on

pseudoviruses. Our investigation indicated that 3E8 might be a powerful broad-spectrum coronavirus blocker.

Our results were also confirmed by live virus study in a BSL-3 laboratory setting. Results showed that incubation with 3E8 inhibited, in a concentration-dependent manner, the replication of SARS-CoV-2 in Vero E6 cells. The virus RBD-targeting B38 antibody, also inhibited SARS-CoV-2 replication, but was 60-fold less potent than 3E8, as suggested by the difference between their IC_{50} values (2.32 vs. 0.04 nM), even though both of them completely abolished SARS-CoV-2 replication at higher concentrations (Fig. 2, B, C).

More importantly, the neutralizing ability of 3E8 was validated in a mouse model of COVID-19. This model was generated by exogenous delivery of hACE2 with Venezuelan equine encephalitis replicon particles, VEEV-VRP-hACE2, and was published previously (*30*). After VEEV-VRP-hACE2 transfection and antibody application, mice were infected with 10^5 PFU of live SARS-CoV-2 via intranasal route, and then viral RNA loads and tissue damages in lungs were examined 3 days post infection. Consistent with our *in vitro* results, application of 3E8 protected lungs from

virus infection, as indicated by approximately 40-fold reduction in lung viral loads (Fig. 3A) and ameliorated tissue damages (Fig. 3B). In comparison, the viral loads in B38-treated mice were only about 5 times lower than that of control mice. Thus, application of 3E8 achieved significantly greater anti-viral effects than that of B38 in the COVID-19 mouse model we employed.

Since ACE2 plays important roles in maintaining blood pressure homeostasis in the renin-angiotensin system, we evaluated the safety risks of 3E8 both *in vitro* and *in vivo*. Our studies with both recombinant ACE2 protein and Vero E6 cells suggested that 3E8 had no effects on ACE2's catalytic activities even at a concentration as high as 666.7 nM (Fig. 4A, B). Furthermore, incubation with 3E8 did not trigger a clear trend of ACE2 degradation in Vero E6 cells, as indicated by Western blot (Fig. 4C). Although 3E8 caused time-dependent internalization of ACE2, the levels of membrane-expressed ACE2 were stabilized after 24 h of 3E8 incubation (Fig. 4D). In limited number of human ACE2 "knock-in" mice, which only express human version of ACE2, injection of 3E8 did not induce noticeable changes in body weights, or blood chemistry profiles (Fig. S3). In addition, there are no obvious difference in shape, size and pathology of

major organs, including hearts, livers, kidneys, spleens and lungs of treated mice (Fig. S3).

To characterize the epitope recognized by 3E8 on ACE2, we solved the Cryo-EM structure of the ACE2-B0AT1 complex bound with 3E8 at an overall resolution of 3.2 Å (Fig. 5A). Each ACE2 molecule in the complex is bound by a 3E8 molecule that extends from the complex like a wing (Fig. 5A). The heavy chain of 3E8 binds to the peptidase domain of ACE2 mainly through polar interactions between the complementarity-determining region (CDR) 2 and 3 of 3E8 and the N-terminal α1 helix of ACE2 (Fig. 5B). The loop between α2 and α3 of ACE2, referred to as Loop2-3, also contribute limited interactions with 3E8. The resolution at the interface was improved to 3.4 Å by applying focused refinement, supporting detailed analysis on the interactions between ACE2 and 3E8. The interface can be divided into two clusters. At cluster 1, the side chains of Asp103 and Arg104 of 3E8 are hydrogen (H) bonded with the main chain of Phe28 in α1 helix of ACE2 and the side chain of Tyr83 in Loop2-3 of ACE2, respectively (Fig. 5C). Meanwhile, the main chain atoms of Asp103 and Asp104 of 3E8 form H-bonds with the side chain of Gln24 of ACE2. At cluster 2, Tyr54 and Tyr102 of

3E8 interact with Lys31 of ACE2 through cation-π interactions, whereas Asn55 and Lys59 of 3E8 interact with His34 of ACE2 and Glu23 and Gln18 of ACE2, respectively, by forming H-bonds between side chains of these residues (Fig. 5D). Structural alignment of the 3E8/ACE2-B0AT1 complex with the previously reported RBD/ACE2-B0AT1 complex reveals clash between 3E8 and RBD of the SARS-CoV-2 S protein at the binding interface with ACE2 (Fig. 5E), providing explanation for the results of competition assays. The binding site of 3E8, SARS-CoV-2, SARS-CoV and HCoV-NL63 on ACE2 were summarized (*31-33*) (Fig. 5F), and the bound ACE2 at His34 together, which suggested that His34 residue might be critical in anti-coronaviruses activity. Evolutionary tree of 3E8 binding site on ACE2 with different species were also analysed, and there was some phylogenetic diversity on some sites, such as 23, 24, 31 and 34.

The mechanism by which 3E8 is more potent and efficacious than RBD-targeting antibody B38 is not yet fully understood. Limited by the sample size, it is premature to conclude that targeting ACE2 is superior to targeting viral RBD in potency and efficacy. B38 is one of the early anti-SARS-CoV-2 antibodies isolated from COVID-19 patients

and due to the urgent nature, it might not be well engineered with respect to affinity and developability. More head-to-head studies with more ACE2- and RBD-targeting molecules are necessary before drawing any conclusion.

Our result indicated that ACE2-Fc (or called ACE2-Ig) fusion protein molecules may act as a "decoy" to interfere coronaviruses from binding to the endogenous ACE2 molecules (Fig. 2). Although ACE2-Fc molecules can be broad-spectrum in theory, their binding affinity (to RBDs), specificity and developability are usually much lower than antibodies. ACE2-Fc was included in our studies as a control and mediocre efficacy was observed *in vitro*. Thus, we believe that ACE2-neutralizing antibody is a more favorable approach than ACE2-fc fusion protein approach.

"Cocktail" or combination therapies have been currently explored in treating COVID-19 (*14*). A combination of 3E8 with antibodies or fusion proteins recognizing different epitopes (e.g., RBD, NTD and/or glycan) on the viral surface, such as RBD, seems a viable option and should be explored.

It is not surprising that no serious side effect or toxicity of 3E8 were observed *in vitro* or in human ACE2 "knock-in" mice. *In vitro*, 3E8 did not affect the catalytic

activities of ACE2 or trigger significant ACE2 down-regulation. Even though ACE2 internalization was overserved, the levels of membrane ACE2 expression were stabilized after 24 h. It is possible that the ACE2 molecules remaining on the membrane were enough to maintain the physiological functions of ACE2-expressing cells. Previous studies showed that ACE2 “knockout” mice were viable and healthy in general, even though the contratile dysfunction was founded (*34*), indicating that ACE2 is not crucial to the survival of animals. Due to limited animal availability, the conclusion from human ACE2 “knock-in” mice should not be overinterpreted. We plan to repeat this study when more animals are commercially available. Moreover, key signs of cardiovascular health, such as pulse pressure and heartbeat rate, cannot be measured in mice. Thus, the side effects and toxicities of 3E8 should be carefully evaluated in non-human primates before moving to the clinic.

To our knowledge, it is the first time that a “pan” anti-coronavirus epitope has ever been disclosed. Current coronavirus-targeting antibodies focus mainly on highly conserved region of RBD, such as 47D11 (*16*) and S309 (*15*). The epitope of 3E8 binding on ACE2 is identified only partially overlapping with that of RBD domain, but

blocked virus infections with remarkable efficiency, demonstrating the extraordinary power of ACE2 targeting strategy. Previously, an neutralizing antibody (4A8) (*35*) was isolated from convalescent COVID-19 patients with binding on the N-terminal domain (NTD) of the SARS-CoV-2 S-protein, but not the RBD. Our results highlighted again the importance of epitope outside or on the verge of RBD/ACE2 interface, and would facilitate future endeavor searching for broad-spectrum anti-coronavirus approaches.

Taken together, by targeting ACE2 with a neutralizing antibody, we achieved broader and more effective suppression against ACE2-depedent coronaviruses without causing any serious side effects or toxicities. Furthermore, we revealed in the first time a broad-spectrum anti-coronavirus epitope on ACE2. Overall, we presented evidence that 3E8 is a promising therapeutic candidate for both current and future coronavirus-triggered epidemics and disclosed the first time a “pan” anti-coronavirus epitope on human ACE2 molecule.

References and notes:

1. C. Drosten *et al.*, Identification of a novel coronavirus in patients with severe acute respiratory syndrome. *N Engl J Med* **348**, 1967-1976 (2003).
2. A. M. Zaki, S. van Boheemen, T. M. Bestebroer, A. D. Osterhaus, R. A. Fouchier, Isolation of a novel coronavirus from a man with pneumonia in Saudi Arabia. *N Engl J Med* **367**, 1814-1820 (2012).

3. F. Wu *et al.*, A new coronavirus associated with human respiratory disease in China. *Nature* **579**, 265-269 (2020).
4. P. Zhou *et al.*, A pneumonia outbreak associated with a new coronavirus of probable bat origin. *Nature* **579**, 270-273 (2020).
5. J. Grein *et al.*, Compassionate Use of Remdesivir for Patients with Severe Covid-19. *N Engl J Med* **382**, 2327-2336 (2020).
6. Y. Wang *et al.*, Remdesivir in adults with severe COVID-19: a randomised, double-blind, placebo-controlled, multicentre trial. *Lancet* **395**, 1569-1578 (2020).
7. J. A. Plante *et al.*, Spike mutation D614G alters SARS-CoV-2 fitness. *Nature*, (2020).
8. Y. Watanabe, J. D. Allen, D. Wrapp, J. S. McLellan, M. Crispin, Site-specific glycan analysis of the SARS-CoV-2 spike. *Science* **369**, 330-333 (2020).
9. Q. Li *et al.*, The Impact of Mutations in SARS-CoV-2 Spike on Viral Infectivity and Antigenicity. *Cell* **182**, 1284-1294.e1289 (2020).
10. H. Zhao *et al.*, A broad-spectrum virus- and host-targeting peptide against respiratory viruses including influenza virus and SARS-CoV-2. *Nat Commun* **11**, 4252 (2020).
11. D. E. Gordon *et al.*, Comparative host-coronavirus protein interaction networks reveal pan-viral disease mechanisms. *Science*, (2020).
12. M. Hoffmann *et al.*, SARS-CoV-2 Cell Entry Depends on ACE2 and TMPRSS2 and Is Blocked by a Clinically Proven Protease Inhibitor. *Cell* **181**, 271-280.e278 (2020).
13. A. C. Walls *et al.*, Structure, Function, and Antigenicity of the SARS-CoV-2 Spike Glycoprotein. *Cell* **181**, 281-292.e286 (2020).
14. A. Baum *et al.*, Antibody cocktail to SARS-CoV-2 spike protein prevents rapid mutational escape seen with individual antibodies. *Science* **369**, 1014-1018 (2020).
15. D. Pinto, Y. J. Park, M. Beltramello, A. C. Walls, M. A. Tortorici, Cross-neutralization of SARS-CoV-2 by a human monoclonal SARS-CoV antibody. **583**, 290-295 (2020).

16. C. Wang *et al.*, A human monoclonal antibody blocking SARS-CoV-2 infection. *Nat Commun* **11**, 2251 (2020).
17. X. Chi *et al.*, A neutralizing human antibody binds to the N-terminal domain of the Spike protein of SARS-CoV-2. *Science* **369**, 650-655 (2020).
18. Y. Wu *et al.*, A noncompeting pair of human neutralizing antibodies block COVID-19 virus binding to its receptor ACE2. *Science* **368**, 1274-1278 (2020).
19. R. A. Santos, F. Frézard, A. J. Ferreira, Angiotensin-(1-7): blood, heart, and blood vessels. *Curr Med Chem Cardiovasc Hematol Agents* **3**, 383-391 (2005).
20. C. M. Ferrario, Angiotensin-converting enzyme 2 and angiotensin-(1-7): an evolving story in cardiovascular regulation. *Hypertension* **47**, 515-521 (2006).
21. W. Li *et al.*, Angiotensin-converting enzyme 2 is a functional receptor for the SARS coronavirus. *Nature* **426**, 450-454 (2003).
22. H. Hofmann *et al.*, Human coronavirus NL63 employs the severe acute respiratory syndrome coronavirus receptor for cellular entry. *Proc Natl Acad Sci U S A* **102**, 7988-7993 (2005).
23. L. van der Hoek *et al.*, Identification of a new human coronavirus. *Nat Med* **10**, 368-373 (2004).
24. G. Y. Oudit *et al.*, SARS-coronavirus modulation of myocardial ACE2 expression and inflammation in patients with SARS. *Eur J Clin Invest* **39**, 618-625 (2009).
25. I. Glowacka *et al.*, Differential downregulation of ACE2 by the spike proteins of severe acute respiratory syndrome coronavirus and human coronavirus NL63. *J Virol* **84**, 1198-1205 (2010).
26. M. J. Moore *et al.*, Retroviruses pseudotyped with the severe acute respiratory syndrome coronavirus spike protein efficiently infect cells expressing angiotensin-converting enzyme 2. *J Virol* **78**, 10628-10635 (2004).
27. K. Kuba *et al.*, A crucial role of angiotensin converting enzyme 2 (ACE2) in SARS coronavirus-induced lung injury. *Nat Med* **11**, 875-879 (2005).

28. P. Towler *et al.*, ACE2 X-ray structures reveal a large hinge-bending motion important for inhibitor binding and catalysis. *J Biol Chem* **279**, 17996-18007 (2004).
29. Y. Wu, F. Wang, A noncompeting pair of human neutralizing antibodies block COVID-19 virus binding to its receptor ACE2. **368**, 1274-1278 (2020).
30. Y.-N. Zhang *et al.*, A mouse model for SARS-CoV-2 infection by exogenous delivery of hACE2 using alphavirus replicon particles. *Cell Research*, (2020).
31. R. Yan *et al.*, Structural basis for the recognition of SARS-CoV-2 by full-length human ACE2. *Science* **367**, 1444-1448 (2020).
32. F. Li, W. Li, M. Farzan, S. C. Harrison, Structure of SARS coronavirus spike receptor-binding domain complexed with receptor. *Science* **309**, 1864-1868 (2005).
33. K. Wu, W. Li, G. Peng, F. Li, Crystal structure of NL63 respiratory coronavirus receptor-binding domain complexed with its human receptor. *Proc Natl Acad Sci U S A* **106**, 19970-19974 (2009).
34. M. A. Crackower *et al.*, Angiotensin-converting enzyme 2 is an essential regulator of heart function. *Nature* **417**, 822-828 (2002).
35. X. Chi, R. Yan, A neutralizing human antibody binds to the N-terminal domain of the Spike protein of SARS-CoV-2. **369**, 650-655 (2020).

Acknowledgements: We thank Dr. Hong Qiu (Shanghai Institute of Materia Medica) for the provision of the eukaryotic codon-optimized SARS-CoV-2 S-protein gene, Dr. Lu Lu (Fudan University) for the provision of the pNL4-3.luc.RE, James C. Wang (Shanghai American School) for technical assistance in helpful discussion and assay development. Cryo-EM facility, the supercomputer center and the mass

spectrometry & metabolomics core facility of Westlake University for providing Cryo-EM support, computing support and mass spectrometry support, respectively.

Funding: This work was supported by the China National Grand S&T Special Project (2019ZX09732002-006), the Strategic Priority Research Program of the Chinese Academy of Sciences (CAS) (XDA12020223 and XDA12020330), the National Natural Science Foundation of China (81872785 and 81673347), Shanghai Municipal Commission of Science and Technology of China (17431904400 and 19YF1457400), the National Key R&D Program (2020YFA0509303), the National Natural Science Foundation of China (projects 31971123, 32022037, 81920108015, 31930059), the Key R&D Program of Zhejiang Province (2020C04001), the SARS-CoV-2 emergency project of the Science and Technology Department of Zhejiang Province (2020C03129), the Leading Innovative and Entrepreneur Team Introduction Program of Hangzhou, Westlake Education Foundation and Tencent Foundation.

Competing interests: Yi-Li Chen, Ganjun Chen and Chunhe Wang are employed by Dartsbio Pharmaceuticals

Supplementary Materials:

Materials and Methods

Fig. S1 to S6

Table S1

369 **References (*Fig. 1-5*)**

Fig. 1. Monoclonal antibody 3E8 bound to His-tagged recombinant human ACE2 and neutralized recombinant S1-subunits from multiple coronaviruses. (A) Binding of 3E8 to His-tagged recombinant human ACE2 protein as measured by ELISA. (B) Binding of 3E8 to His-tagged human ACE2 as measured by BLI. (C) Bindings of recombinant S1-subunits from four different coronaviruses to recombinant human ACE2 protein as measured by ELISA. (D) Bindings of recombinant S1-subunits from different coronaviruses to recombinant human ACE2 protein were neutralized by 3E8. (E) The EC_{50} values of recombinant viral S1-subunit bindings to human ACE2 and IC_{50} values of 3E8 in neutralizing S1-subunit/ACE2 bindings.

Fig. 2. 3E8 neutralized cellular infection from pseudo-typed and live coronaviruses *in vitro*. ACE2-Fc and B38 were used as positive controls, and human IgG4 isotype was negative control. (A) 3E8 neutralized the infections of ACE2-overexpressing HEK293 cells by four different pseudo-typed coronaviruses constructed with Env-defective HIV-1 and full-length S-proteins from SARS-CoV-2-D614G,

SARS-CoV-2, SARS-CoV and HCoV-NL63. (B) 3E8 neutralized the infection of Vero E6 cells by live SARS-CoV-2 virus. (C) The IC_{50} values of 3E8 neutralization.

Fig. 3. 3E8 protected animals from live SARS-Cov-2 infection in a mouse model of COVID-19. (A) Application of 3E8 significantly reduced the viral RNA loads in the lungs of BALB/c mice ectopically expressing human ACE2 and inoculated with live SARS-CoV-2 virus. RBD-targeting monoclonal antibody B38 and isotype were used as positive and negative controls, respectively. (B) H&E staining of lung organ samples from different treatment groups. PBS- and isotype-treated mice developed serious interstitial pneumonia characterized with large area of alveolar septal thickening, large number of inflammatory cell infiltration (black arrow), even formed vascular cuff around blood vessels (yellow arrow), bleeding areas (blue arrow), and material exudates from the alveolar cavity (green arrow). B38-treated mice showed slightly-less histological pneumonia than the two groups. Only inflammatory cell infiltration (black arrow) and formed vascular cuff around blood vessels (yellow arrow) were observed in the lungs of 3E8-treated mice. The scale represents 100 μm. *: $p<0.05$; **: $p<0.01$.

Fig. 4. 3E8-treatment showed no effects on ACE2's physiological functions. (A) 3E8 treatment showed no effect on enzymatic activities of recombinant human ACE2 protein. AF933, an ACE2 polyclonal goat antibody, was used as positive control. Sera from non-immune mice, hIgG1-Fc and isotype were used as negative controls. (B) 3E8 treatment showed no effects on the enzymatic activity of ACE2 molecules endogenously expressed on Vero E6 cells. (C) Total expression of ACE2 by Vero E6 cells was not affected by 3E8 treatment at 0.133, 0.667 and 6.67 nM for 24 h. (D) The levels of membrane ACE2 on HEK293 cells was reduced by 3E8 treatment but stabilized after 24 h. *: $p<0.05$; **: $p<0.01$.

Fig. 5 Cryo-EM structure of the 3E8/ACE2-B^{0}AT1 complex and interactions between 3E8 and ACE2. Domain-colored Cryo-EM map (A, upper left panel) and the side view (A, upper right panel) or the top view (A, lower panel) of the structure. The heavy and light chains of 3E8 are colored green and violet, respectively. The ACE2 and B^{0}AT1 are colored cyan and wheat, respectively. (B) Binding interface between 3E8 and ACE2, which contains two clusters that are labeled with red and black dashed ellipses and detailed shown in (C) and (D), respectively. H-bonds are

indicated by red dashed lines. (E) Structural alignment of the 3E8/ACE2-B^0AT1 complex and the RBD/ACE2-B^0AT1 complex (PDB ID: 6M17) shows clash between 3E8 and RBD of the SARS-CoV-2 S protein. (F) Summary of binding site of multiple coronaviruses on ACE2. (G) Evolutionary tree of 3E8 binding site on ACE2 with different species.

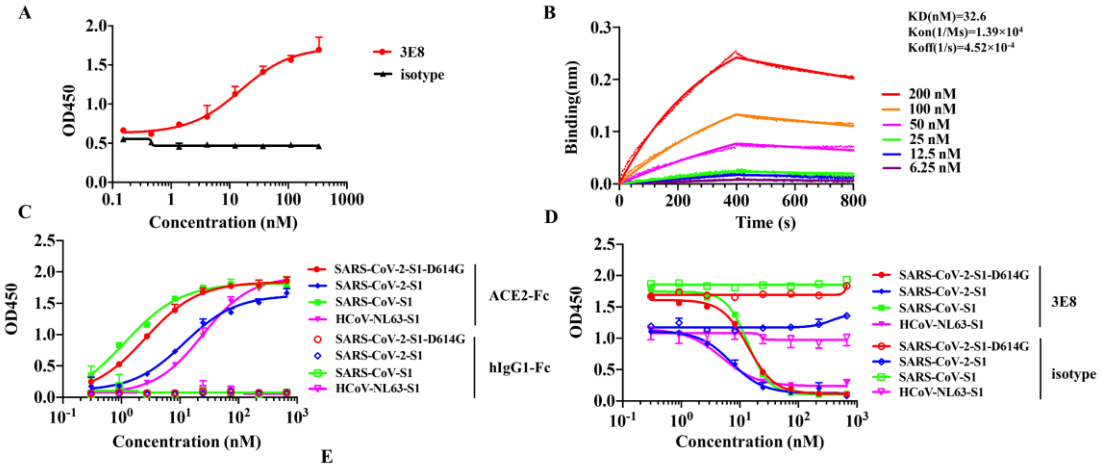

E

S1 proteins	S1-ACE2 binding (nM)	
	EC_{50}	Neutralization of 3E8 (IC_{50})
SARS-CoV-2-S1-D614G	2.579	13.80
SARS-CoV-2-S1	11.82	7.116
SARS-CoV-S1	1.132	13.73
HCoV-NL63-S1	24.24	4.957

Fig. 1

371

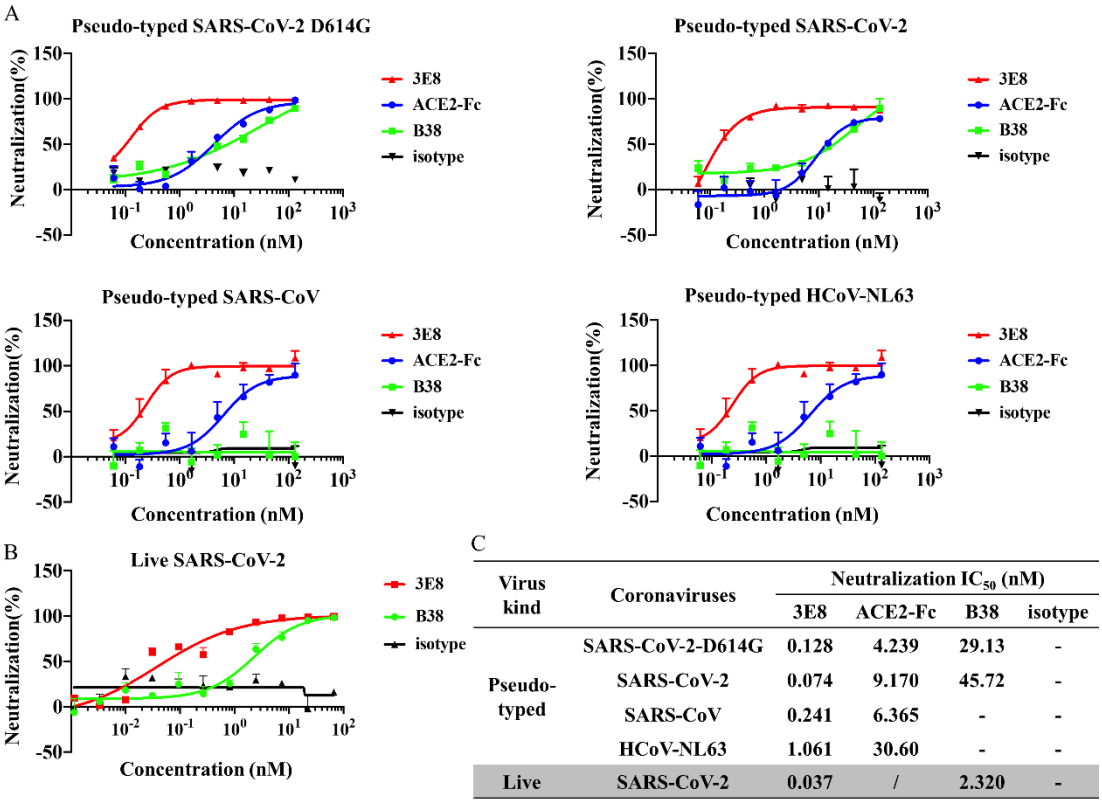

C

Virus kind	Coronaviruses	Neutralization IC_{50} (nM)			
		3E8	ACE2-Fc	B38	isotype
Pseudo-typed	SARS-CoV-2-D614G	0.128	4.239	29.13	-
	SARS-CoV-2	0.074	9.170	45.72	-
	SARS-CoV	0.241	6.365	-	-
	HCoV-NL63	1.061	30.60	-	-
Live	SARS-CoV-2	0.037	/	2.320	-

Fig. 2

372

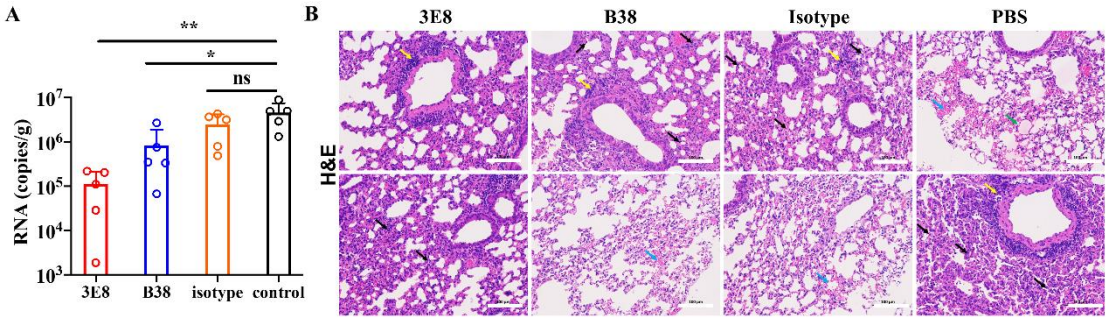
A
**
*
ns
RNA (copies/g)
10^7
10^6
10^5
10^4
10^3
3E8
B38
isotype
control
B
3E8
B38
Isotype
PBS
H&E

Fig. 3

373

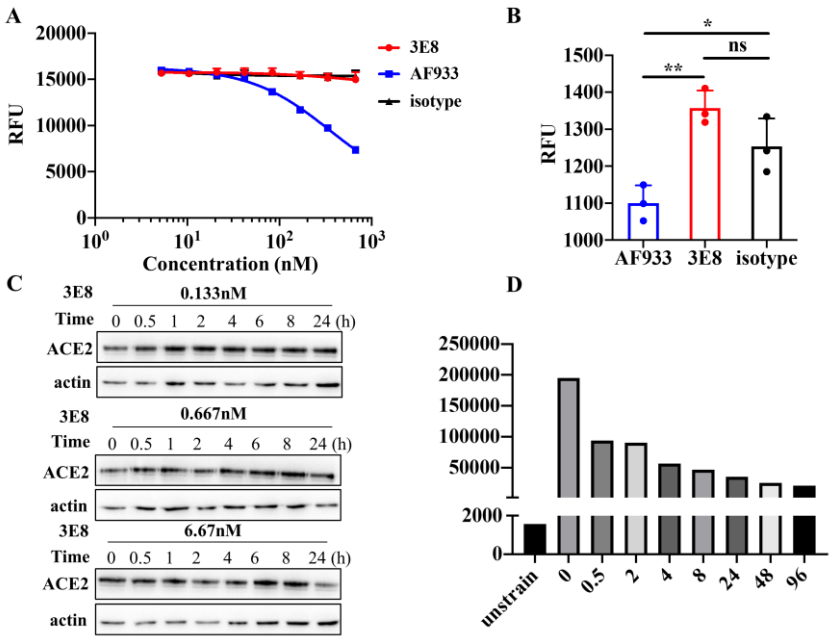
A
20000
15000
10000
5000
0
RFU
10^0
10^1
10^2
10^3
Concentration (nM)
3E8
AF933
isotype
B
1500
1400
1300
1200
1100
1000
RFU
*
ns
**
AF933
3E8
isotype
C
3E8
0.133nM
Time
0 0.5 1 2 4 6 8 24 (h)
ACE2
actin
3E8
0.667nM
Time
0 0.5 1 2 4 6 8 24 (h)
ACE2
actin
3E8
6.67nM
Time
0 0.5 1 2 4 6 8 24 (h)
ACE2
actin
D
250000
200000
150000
100000
50000
2000
0
unstrain
0
0.5
2
4
8
24
48
96

Fig. 4

374

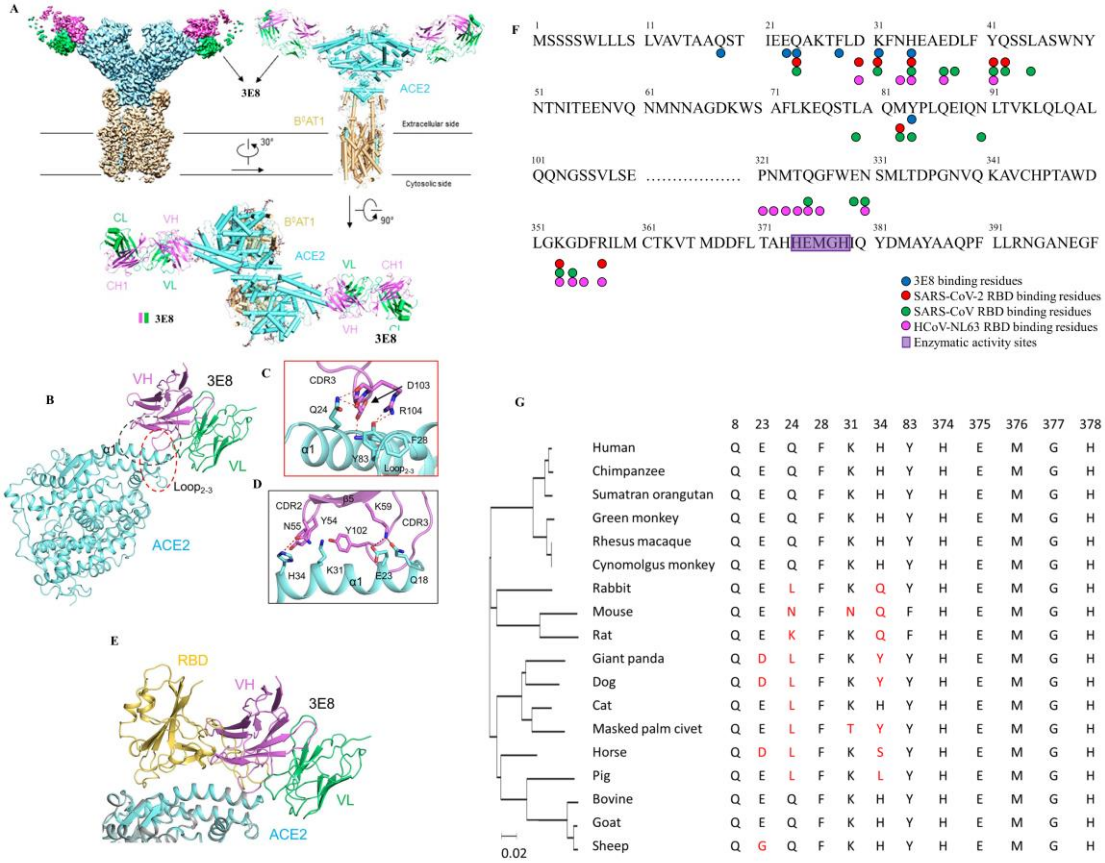
A
3E8
ACE2
B⁰AT1
Extracellular side
Cytosolic side
30°
90°
CL
VH
CH1
VL
3E8
B
VH
3E8
α1
VL
Loop2-3
ACE2
C
CDR3
D103
Q24
R104
F28
α1
Y83
Loop2-3
D
CDR2
β5
K59
N55
Y54
Y102
CDR3
H34
K31
α1
E23
Q18
E
RBD
VH
3E8
VL
ACE2
F
MSSSSWLLLS LVAVTAAQST IEEQAKTFLD KFNHEAEDLF YQSSLASWNY
NTNITEENVQ NMNNAGDKWS AFLKEQSTLA QMYPLQEIQN LTVKLQLQAL
QQNGSSVLSE …… PNMTQGFWEN SMLTDPGNVQ KAVCHPTAWD
LGKGDFRILM CTKVT MDDFL TAHHEMGHIQ YDMAYAAQPF LLRNGANEGF
3E8 binding residues
SARS-CoV-2 RBD binding residues
SARS-CoV RBD binding residues
HCoV-NL63 RBD binding residues
Enzymatic activity sites
G
8 23 24 28 31 34 83 374 375 376 377 378
Human Q E Q F K H Y H E M G H
Chimpanzee Q E Q F K H Y H E M G H
Sumatran orangutan Q E Q F K H Y H E M G H
Green monkey Q E Q F K H Y H E M G H
Rhesus macaque Q E Q F K H Y H E M G H
Cynomolgus monkey Q E Q F K H Y H E M G H
Rabbit Q E L F K Q Y H E M G H
Mouse Q E N F N Q F H E M G H
Rat Q E K F K Q F H E M G H
Giant panda Q D L F K Y Y H E M G H
Dog Q D L F K Y Y H E M G H
Cat Q E L F K H Y H E M G H
Masked palm civet Q E L F T Y Y H E M G H
Horse Q D L F K S Y H E M G H
Pig Q E L F K L Y H E M G H
Bovine Q E Q F K H Y H E M G H
Goat Q E Q F K H Y H E M G H
Sheep Q G Q F K H Y H E M G H
0.02

Fig. 5

375